THE JOURNAL OF BIOLOGICAL CHEMISTRY VOL. 281, NO. 10, pp. 6682–6690, March 10, 2006

Single Amino Acid Mutations Alter the Distribution of Human Porphobilinogen Synthase Quaternary Structure Isoforms (Morpheeins)*

Received for publication, October 12, 2005, and in revised form, November 29, 2005 Published, JBC Papers in Press, December 23, 2005, DOI 10.1074/jbc.M511134200

Lei Tang[‡], Sabine Breinig[‡], Linda Stith[‡], Adele Mischel[‡], Justin Tannir[‡], Bashkim Kokona[§], Robert Fairman[§], and Eileen K. Jaffe[‡1]

From the [‡]Fox Chase Cancer Center, Philadelphia, Pennsylvania 19111 and the [§]Biology Department, Haverford College, Haverford, Pennsylvania 19041

Porphobilinogen synthase (PBGS) is an obligate oligomer that can exist in functionally distinct quaternary states of different stoichiometries, which are called morpheeins. The morpheein concept describes an ensemble of quaternary structure isoforms wherein different structures of the monomer dictate different multiplicities of the oligomer (Jaffe, E. K. (2005) *Trends Biochem. Sci.* 30, 490–497). Human PBGS assembles into long-lived morpheeins and has been shown to be capable of forming either a high activity octamer or a low activity hexamer (Breinig, S., Kervinen, J., Stith, L., Wasson, A. S., Fairman, R., Wlodawer, A., Zdanov, A., and Jaffe, E. K. (2003) *Nat. Struct. Biol.* 10, 757–763). All PBGS monomers contain an $\alpha\beta$-barrel domain and an N-terminal arm domain. The N-terminal arm structure varies among PBGS morpheeins, and the spatial relationship between the arm and the barrel dictates the different quaternary assemblies. We have analyzed the structures of human PBGS morpheeins for key interactions that would be predicted to affect the oligomeric assembly. Examples of individual mutations that shift assembly of human PBGS away from the native octamer are R240A and W19A. The alternate morpheeins of human PBGS variants R240A and W19A are chromatographically separable from each other and kinetically distinct; their structure and dynamics have been characterized by native gel electrophoresis, dynamic light scattering, and analytical ultracentrifugation. R240A assembles into a metastable hexamer, which can undergo a reversible conversion to the octamer in the presence of substrate. The metastable nature of the R240A hexamer supports the hypothesis that octameric and hexameric morpheeins of PBGS are very close in energy. W19A assembles into a mixture of dimers, which appear to be stable.

Evidence is building to support the notion that the porphobilinogen synthase (PBGS[2]; EC 4.2.1.24) family of enzymes can exist as an equilibrium of quaternary structure isoforms, denoted morpheeins (1–3). Morpheeins comprise an equilibrium ensemble of protein structures wherein a protein monomer can exist in more than one conformation, and each monomer conformation dictates a functionally different quaternary structure of finite multiplicity. Morpheeins have been proposed to provide a structural foundation for allosteric regulation, cooperativity, and hysteresis in some proteins (2). As such, the energetic difference between morpheeins of a given protein must be small. The propensity of PBGS to assume various morpheein structures and the rates of PBGS morpheein interconversion are highly species-dependent. The stable morpheeins of human PBGS are the octamer, found for the wild-type protein, and the hexamer, first seen for the naturally occurring mutation F12L (1). Coexpression of human wild-type PBGS and F12L generates a population of PBGS proteins composed of hetero-octamers and hetero-hexamers, each of which contains a mixture of Phe^{12}- and Leu^{12}-containing chains (1). The structure and composition of these hetero-oligomers are stable during storage, but the molecular motions resulting from catalysis favor formation of the octamer with an accompanying disproportionation of Phe^{12}-containing chains into the octamer (3). The remaining hexamer has an increased proportion of Leu^{12}-containing chains (3). The physical basis for the thermodynamic propensity of Leu^{12}-containing chains to form the hexamer remains unclear, but examination of the structure of human PBGS suggests that other single amino acid mutations might affect the folding and assembly of the protein to favor structures other than the octamer.

In this study, we report on alterations of two amino acids (Arg^{240} and Trp^{19}) that were chosen based on an analysis of the structures and subunit interactions seen in human octameric and hexameric PBGS, for which the assemblies are shown in Fig. 1. Each human PBGS subunit is composed of a 306-amino acid TIM-like $\alpha\beta$-barrel and a 24-amino acid N-terminal arm. The conformational difference between the monomer that assembles into the octamer and the monomer that assembles into the hexamer is a dramatic reorientation of the arm with respect to the barrel; for the F12L hexamer, this reorientation occurs at Thr^{23}. In both the octameric and hexameric assemblies, two monomers come together to form a dimer with a conserved barrel-barrel interface. The dimer that assembles into the octamer is called a hugging dimer (Fig. 1*a*), whereas the dimer that assembles into the hexamer is called a detached dimer (Fig. 1*b*) (1). The difference between these two dimers is the presence or absence of a "hugging" interaction between the N-terminal arm of one subunit and the $\alpha\beta$-barrel of the adjacent subunit of the dimer.

The "arm-hugging-barrel" interaction of PBGSs from plants, Archaea, and most Bacteria is stabilized by an allosteric magnesium (Fig. 2*a*), which has been seen in the crystal structures of PBGSs from *Pseudomonas aeruginosa* (4) and *Escherichia coli* (5) and which has been shown to facilitate the formation of the octamer (1, 6). PBGSs from animals and yeast do not contain an allosteric magnesium-binding site

* This work was supported by National Institutes of Health Grants ES03654 (to E. K. J.), and CA006927 (to the Institute for Cancer Research, Fox Chase Cancer Center); by National Science Foundation Grant MCB-0211754 (to R. F); by an appropriation from the Commonwealth of Pennsylvania; and by the Pennsylvania Department of Health. The costs of publication of this article were defrayed in part by the payment of page charges. This article must therefore be hereby marked "*advertisement*" in accordance with 18 U.S.C. Section 1734 solely to indicate this fact.

[1] To whom correspondence should be addressed: Fox Chase Cancer Center, 333 Cottman Ave., Philadelphia, PA 19111. Tel.: 215-728-3695; Fax: 215-728-2412; E-mail: Eileen.Jaffe@fccc.edu.

[2] The abbreviations used are: PBGS, porphobilinogen synthase; β-ME, β-mercaptoethanol; ALA, 5-aminolevulinic acid; bis-tris propane-HCl, 1,3-bis(tris(hydroxymethyl)-methylamino)propane hydrochloride.

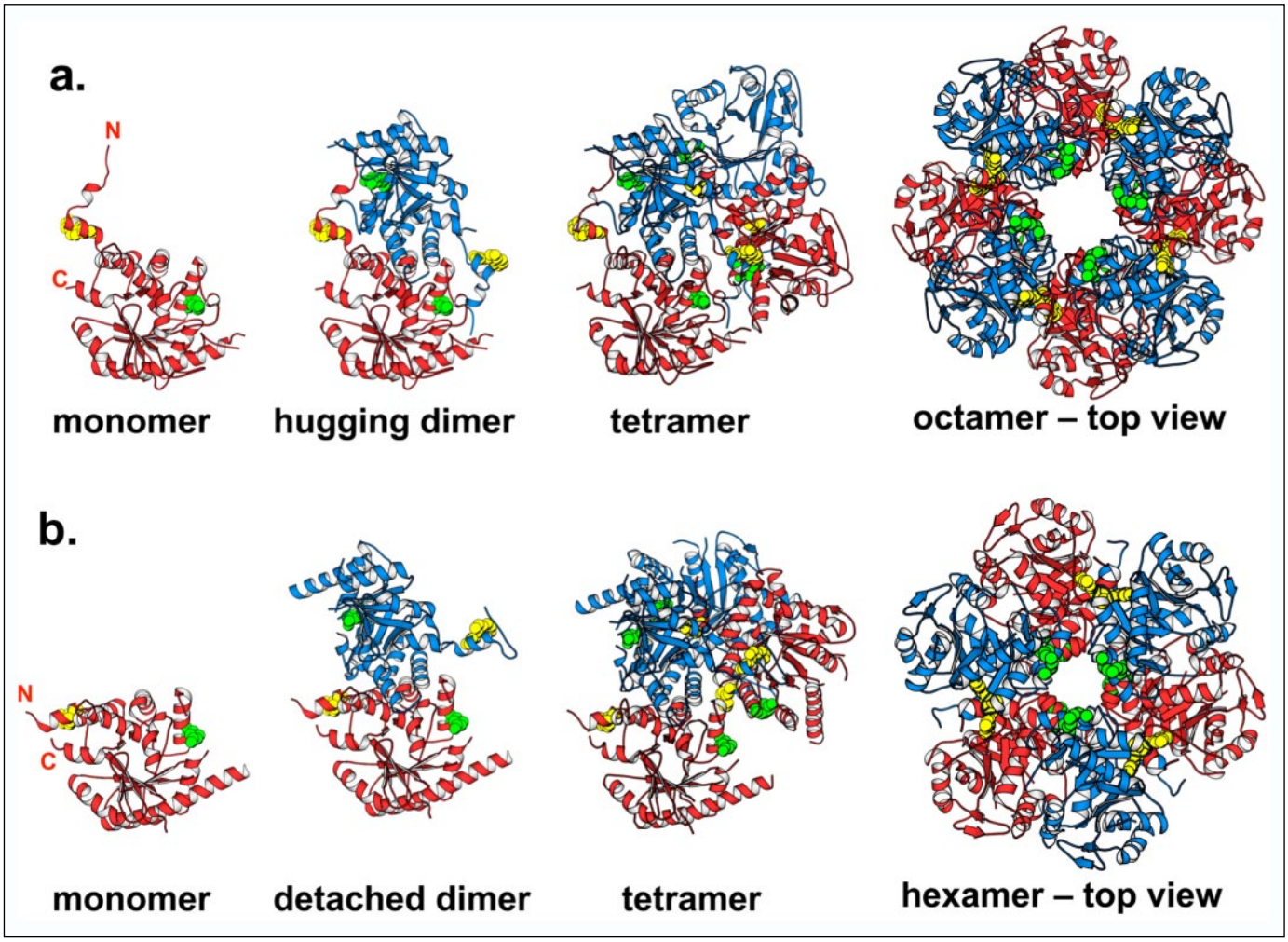

FIGURE 1. **Assembly of the human PBGS quaternary structure isoforms.** The subunits of each homodimer are colored *red* and *blue* for clarity. Trp^{19} (*yellow*) and Arg^{240} (*green*) are shown in space-filling representation. N and C termini are labeled on the monomer. Other apparent chain breaks are due to disordered regions of the protein. *a*, assembly of the octamer (Protein Data Bank code 1E51) showing (*left* to *right*) the monomer, the hugging dimer, the tetramer, and a top view of the octamer. *b*, assembly of the hexamer (Protein Data Bank code 1PV8) showing (*left* to *right*) the monomer, the detached dimer, the tetramer, and a top view of the hexamer.

(7). Instead, the guanidinium group of an arginine (Arg^{240} of human PBGS) is spatially equivalent to the allosteric magnesium of those non-human PBGSs (Fig. 2*b*). Arg^{240} does not interact with the arm in the hexameric assembly (Fig. 2*c*). We posit that Arg^{240} provides stabilization for the human PBGS octamer via hydrogen-bonding interactions with Ser^5 of the adjacent chain and that the human PBGS mutant R240A would fold and assemble into a hexamer. Herein, this hypothesis is proven to be correct. However, substrate binding and turnover are shown to favor re-equilibration into the octameric assembly, which demonstrates that the energy difference between these two morpheeins is small.

A second hypothesis relates to a dimer-dimer interface that is common to both the hexameric and octameric assemblies of human PBGS. This interaction snuggles the N-terminal arm of the upper subunit of the first dimer against the bottom face of the $\alpha\beta$-barrel of the lower subunit of the second dimer (Fig. 3). Unlike the hugging interface dominated by Arg^{240}, which has considerable hydrophilic character, the "snuggling" interface is more hydrophobic in nature and is dominated by the penetration of the barrel by Trp^{19} of the arm. Therefore, we posit that a W19A mutation will destabilize both the octameric and hexameric assemblies. Herein, we establish that the human PBGS mutant W19A is dimeric. However, more than one dimeric structure is formed, and these dimers do not readily interconvert. The sum of the data on the human PBGS mutant F12L, which occurs naturally, and the synthetic mutants R240A and W19A demonstrate that there are single amino acid mutations in different parts of human PBGS that can dramatically destabilize the folding and assembly away from the native octameric state, yet some mutations allow interconversion between morpheein forms.

EXPERIMENTAL PROCEDURES

Mutagenesis and Protein Purification—Mutagenesis was performed using the QuikChange site-directed mutagenesis kit (Qiagen Inc.) starting with a pET3a-based plasmid containing the synthetic gene for the human wild-type PBGS variant N59(C162A) (8). The primers used to generate the R240A variant were 5′-CCGTGCTGTGGAC**GCA**GATGTACGGGAAGGCGC-3′ and 3′-GCGCCTTCCCGTACATC**TG**-**C**GTCCACAGCACGG-5′. The primers used to generate the W19A variant were 5′-CCACTGCTTCGGGCC**GCC**CAGACAGCCACC-3′ and 3′-GGTGGCTGTCTG**GGC**GGCCCGAAGCAGTGG-5′. All mutant sequences were confirmed throughout the gene in both directions.

For protein production, the plasmids encoding R240A and W19A were transformed into *E. coli* BLR(DE3) cells and plated on Luria broth plates with 0.4% glucose, 100 μg/ml ampicillin, and 12.5 μg/ml tetracycline. Following overnight incubation, single colonies were each inocu-

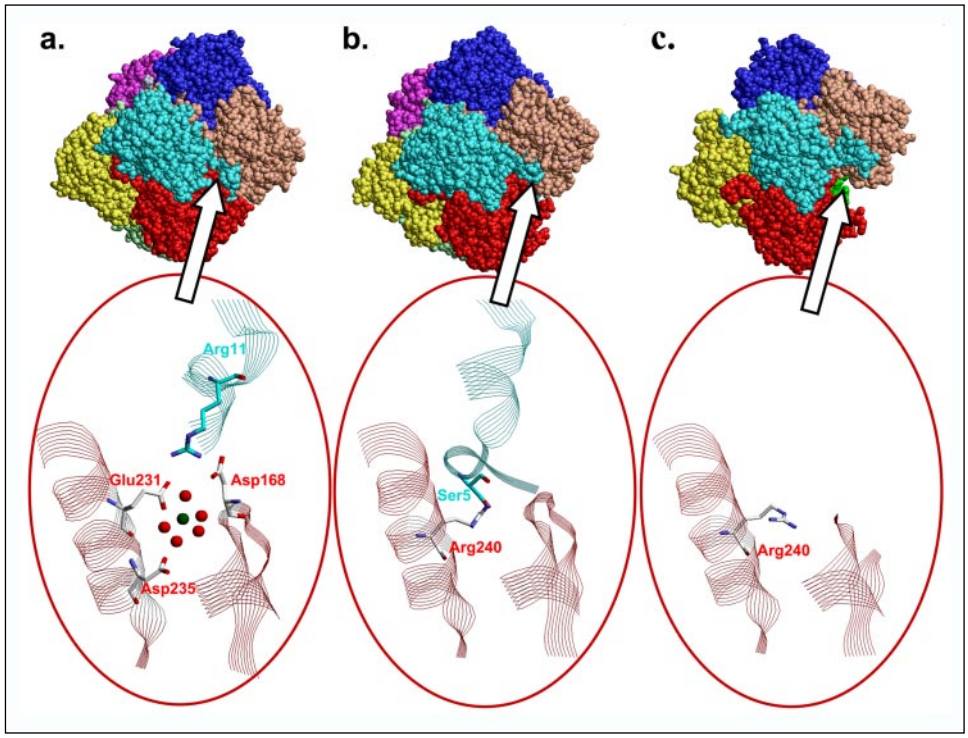

FIGURE 2. **Spatial and structural equivalence of Arg^{240} to the allosteric Mg^{2+} of other PBGSs.** *a*, the octamer of *E. coli* PBGS (Protein Data Bank code 1L6S) is shown in space-filling representation colored by subunit. The enlargement shows the allosteric Mg^{2+} (*green*) at the arm-barrel interface. Included are the five first coordination sphere water ligands (*red balls*) and the residues whose side chains contribute to the Mg^{2+} coordination. Strands are depicted for residues 162–172 and 226–240 (*red* subunit) and for residues 8–15 (*cyan* subunit). *b*, the octamer of human PBGS (Protein Data Bank code 1E51, which lacks coordinates for protein-associated water) is shown as described for *a*. The enlargement shows Arg^{240} (*red* subunit), which is hydrogen-bonded to the backbone carbonyl of Ser^5 (*cyan* subunit). Strands are depicted for residues 165–177 and 232–246 (*red* subunit) and residues 1–14 (*cyan* subunit). *c*, the hexamer of the human PBGS mutant F12L (Protein Data Bank code 1PV8) is shown as described for *a*. The enlargement shows Arg^{240} (*red* subunit) and the strands corresponding to the enlargement in *b*. The *cyan* subunit, which is reoriented in the hexamer, is well outside the enlarged region; sections of region 165–177 are disordered, and there are no ordered water molecules within 3.2 Å of Arg^{240}.

lated into 1 liter of Luria broth with 0.4% glucose, 100 μg/ml ampicillin, and 12.5 μg/ml tetracycline. Cells were harvested after overnight shaking at 37 °C and then resuspended in fresh medium containing 20 μM $ZnCl_2$, 100 μg/ml ampicillin, and 12.5 μg/ml tetracycline at 15 °C. After 1 h, isopropyl β-D-thiogalactopyranoside was added to a final concentration of 100 μM to induce slow protein expression for an additional 20 h at 15 °C. Cells (6–9 g/liter) were harvested, frozen using liquid nitrogen, and stored at −80 °C.

Harvested cells were suspended in potassium phosphate buffer, lysed with lysozyme in the presence of DNase I enzyme, sonicated, and the soluble protein was subjected to 20–45% ammonium sulfate fractionation as described previously (8). The 45% saturated ammonium sulfate pellet was dissolved in 30 mM potassium phosphate (pH 7.0), 15% saturated ammonium sulfate, 10 mM β-mercaptoethanol (β-ME), 10 μM $ZnCl_2$, and 0.1 mM phenylmethylsulfonyl fluoride and applied to a phenyl-Sepharose column (50 ml) that had been equilibrated with the same buffer. The column was washed with the same buffer for 1 column volume, followed by a 10-column volume linear gradient of 30 to 2 mM potassium phosphate (pH 7.0), 15 to 0% saturated ammonium sulfate, 10 mM β-ME, 10 μM $ZnCl_2$, and 0.1 mM phenylmethylsulfonyl fluoride. Human PBGS mutants eluted near the end of or after the gradient in a 1-column volume wash with the ending buffer. The eluted protein was applied to a Q-Sepharose column (~80-ml column volume) that had been equilibrated with 30 mM potassium phosphate (pH 7.5), 10 mM β-ME, 10 μM $ZnCl_2$, and 0.1 mM phenylmethylsulfonyl fluoride. A nonlinear salt gradient in the same buffer base (3.4 column volumes without KCl and then a 4.2-column volume linear gradient to 0.18 M KCl, followed by 0.18 M KCl for an additional 4.8 column volumes) provided a base-line separation of the various morpheeins of human PBGS. The Q-Sepharose column was regenerated with a 2.6-column volume linear gradient from 0.18 to 0.36 M KCl and then rapidly returned to and equilibrated with the initial equilibration buffer. The characteristics of various pools from the Q-Sepharose column are reported herein. In some cases, protein was pooled and concentrated to ~10 mg/ml by ultrafiltration using Centriprep-10 concentration devices, and 5 ml were applied to a 320-ml Sephacryl S-300 column equilibrated and eluted with 0.1 M potassium phosphate (pH 7), 10 mM β-ME, and 10 μM $ZnCl_2$ at a flow rate of 1 ml/min. Protein concentration was determined

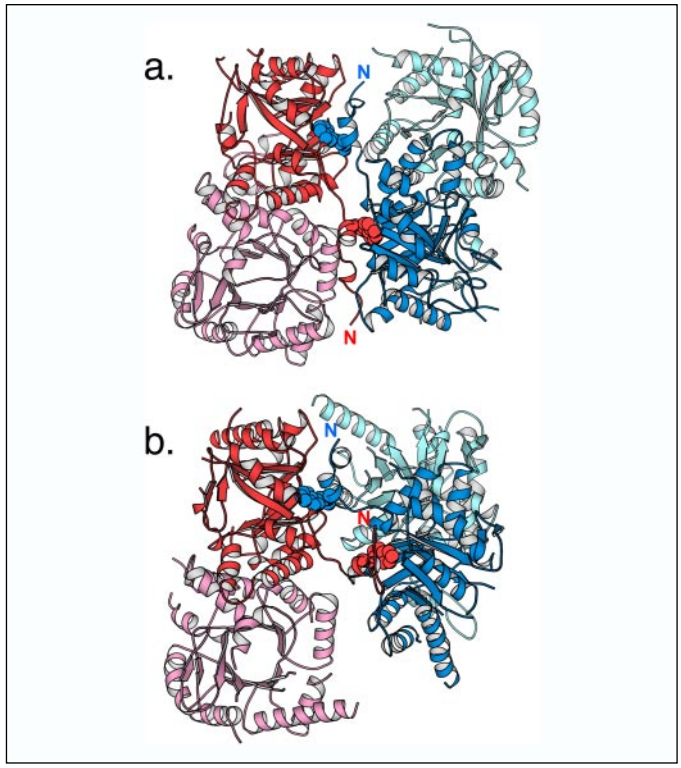

FIGURE 3. **Location of Trp^{19} in human PBGS.** *a*, the penetration of Trp^{19} (*red* space-filling representation) of the upper subunit of the first hugging dimer into the $\alpha\beta$-barrel of the lower subunit of the second hugging dimer in an octameric assembly of human PBGS. The reciprocal interaction is also shown (*blue* space-filling representation). *b*, the penetration of Trp^{19} (*red* space-filling representation) of the upper subunit of the first detached dimer into the $\alpha\beta$-barrel of the lower subunit of the second detached dimer in a hexameric assembly of human PBGS. The reciprocal interaction is also shown (*blue* space-filling representation).

by the Bradford assay (Pierce) using bovine serum albumin as the standard. Purified proteins were pooled, concentrated, aliquoted, flash-frozen in liquid nitrogen, and stored at −80 °C.

Specific Activity Determination of the Human PBGS Mutants—The enzyme activity was determined based on the formation of porphobilinogen from 5-aminolevulinic acid (ALA) as follows. Proteins were preincubated at 37 °C for 10 min in assay buffer composed of 0.1 M bis-tris propane-HCl at desired pH values, 10 mM β-ME, and 10 μM $ZnCl_2$. ALA-HCl was then added to a final concentration of 10 mM with a concomitant drop in the pH to the reported value. The 1-ml reaction solutions were incubated at 37 °C for 5 min to several hours. Reactions were stopped by the addition of 0.5 ml of STOP reagent (20% trichloroacetic acid and 0.1 M $HgCl_2$), followed by vigorous vortexing. The stopped assay solutions were centrifuged at 5000 rpm for 3 min to remove the precipitated protein and β-ME. 0.8 ml of clarified stopped assay solution were mixed with 0.8 ml of Ehrlich's reagent (2 g of dimethylaminobenzaldehyde dissolved in 20 ml of 70% perchloric acid and then brought to 100 ml with glacial acetic acid) with vigorous vortexing. Porphobilinogen formation was determined by the absorbance at 555 nm (ϵ_{555} = 60,200 M^{-1} cm^{-1} (9)) after 8 min of pink color development. If the absorbance was above 1.0, the stopped assay mixture was diluted into a solution of 1 part STOP reagent and 2 parts assay buffer prior to development of 0.8 ml of this mixture with 0.8 ml of Ehrlich's reagent.

Kinetic Characterization of the Human PBGS Mutants—The pH-rate profiles were measured using 0.1 M bis-tris propane-HCl over a wide range of pH values. The reported pH values reflect the final pH in the assay solution after the addition of ALA-HCl to a final concentration of 10 mM. For K_m and V_{max} determination, ALA-HCl concentrations were 10 μM, 30 μM, 100 μM, 300 μM, 1 mM, 3 mM, and 10 mM, retaining a total HCl concentration of 10 mM to obtain a constant final pH. Protein concentration dependence at pH 9 for R240A and W19A was measured at a range of 0.3–100 μg/ml for each PBGS mutant using bis-tris propane-HCl buffer. Four different ALA-HCl concentrations were used: 1, 3, 6, and 10 mM.

Analytical Ultracentrifugation—W19A (0.29 mg/ml) was dialyzed into 30 mM potassium phosphate (pH 7.5), 0.1 mM dithiothreitol (Roche Applied Science), and 10 μM $ZnCl_2$. R240A (0.24 mg/ml) was dialyzed into 30 mM potassium phosphate, 0.1 mM dithiothreitol, and 10 μM $ZnCl_2$ at pH 7 and 9. The proteins were dialyzed overnight into fresh buffer prior to the sedimentation equilibrium experiment to avoid any aggregation as result of cysteine oxidation. Sedimentation equilibrium experiments were carried out at 4 °C using a Beckman Optima XL-A analytical ultracentrifuge as described previously (10). Temperature-corrected partial specific volumes and solution density calculations were performed using the Sednterp program (11); 110 μl of sample and 125 μl of buffer were loaded into a six-sectored Epon charcoal-filled centerpiece, and data were collected at 291 nm. Samples were run at 4 °C at rotor speeds of 8000, 11,000, 14,000, and 18,000 rpm with delay conditions of 12 h to ensure equilibrium. The molecular masses of W19A (36,134 Da) and R240A (36,164 Da) were determined based on the amino acid sequence using Sednterp. Data analysis was performed using WinNonlin software (Version 1.037) (12).

Native Gel Electrophoresis—Electrophoresis was performed using a PhastGel system (Amersham Biosciences) with PhastGel native buffer strips (0.88 M L-alanine and 0.25 M Tris (pH 8.8), made of 3% Agarose IEF). Protein samples were mixed with native gel running buffer (0.1 M Tris-HCl (pH 8.8), 20% glycerol, and 0.0025% bromphenol blue) to a final concentration of ~1 mg/ml. Four microliters of each sample were loaded onto a homogeneous 12.5% polyacrylamide gel (12.5% total acrylamide in the separation zone; buffer of 0.112 M acetate and 0.112 M Tris at pH 6.5). After separation, gels were developed on the PhastGel system using Coomassie Blue staining.

Equilibrium Dialysis Experiments—Equilibrium dialysis experiments were carried out at 37 °C with gentle agitation (50–60 rpm) in an air shaker. The dialysis buffer was 0.1 M bis-tris propane-HCl at desired pH values, 10 mM β-ME, and 10 μM $ZnCl_2$ with or without 10 mM ALA-HCl. The reported pH values reflect the buffer pH after the addition of ALA-HCl (when included). R240A (~400 μl, 1.8 mg/ml) or W19A (~350 μl, 6 mg/ml) solutions were dialyzed against 300 ml of buffer for 24 h or longer. The formation of porphobilinogen in the dialysis buffer was monitored periodically by reaction of a sample of the buffer with STOP reagent and Ehrlich's reagent (see above). Protein samples were taken from the dialysis cassettes (Slide-A-Lyzer dialysis cassette, Pierce) at the desired time points for native gel electrophoresis. Gels were scanned, and the fractional intensity of total octameric protein at each time point was quantified using SigmaGel™ gel analysis software (Jandel Corp.).

Dynamic Light Scattering Measurement—Measurements were carried out using a temperature-controlled DynaPro dynamic light scattering instrument (Protein Solutions Inc.) at 37 °C. A protein solution (~1 mg/ml) was preincubated in assay buffer at 37 °C for 10 min and then filtered through a 0.2-μm membrane into a 37 °C prewarmed light scattering cuvette. The average molecular masses were calculated based on the measurements of Kc/R90 (13).

RESULTS

Analysis of the newly prepared variants was based on prior experience with human PBGS octameric and hexameric proteins, which vary dramatically in their pH activity profiles, K_m values, migration on native gel electrophoresis, elution from ion exchange columns, and behavior upon analytical ultracentrifugation (1–3). Our gel electrophoresis standards for the octamer and hexamer are the wild-type protein and F12L, respectively.

Human PBGS Mutant R240A—The purification of R240A followed a reported procedure (3) through the Q-Sepharose column step, where two major peaks of protein exhibited PBGS activity (Fig. 4*a*). The first peak to elute (fractions 59–65, Pool I, ~150 mg) appeared at the retention time of hexameric F12L, ran comparably with hexameric F12L on a native gel, and had enhanced activity at pH 9 relative to pH 7 (Fig. 4*a*) also like hexameric F12L. The pH-rate profile of this hexameric form of R240A (Fig. 4*b*) mirrors that of hexameric human PBGS (1, 3). This pool was further purified on Sephacryl S-300 and retained the same pH-rate profile. Analytical ultracentrifugation and dynamic light scattering measurements confirmed the hexameric state of this Sephacryl S-300-purified R240A. The global fit to the analytical ultracentrifugation data (loading concentration of 0.24 mg/ml) suggests an apparent molecular mass that is between those of a pentamer and hexamer and independent of the buffer pH (Table 1). The best two-state model is that of a dimer in equilibrium with a hexamer where the hexamer predominates the mixture, constituting up to 80% by weight. At a concentration of 1 mg/ml, dynamic light scattering measurements indicated an apparent molecular mass corresponding to a hexamer at pH 7 (Table 1).

The second peak of R240A from the Q-Sepharose column (Pool II) (Fig. 4*a*) was broad and encompassed the retention time of human wild-type octameric PBGS. Pool II was analyzed over several days and behaved in a time-dependent fashion like a mixture of octameric and hexameric PBGS as determined on native gels and by a variable ratio of activity at pH 7 relative to pH 9. Pool II was concentrated 10-fold,

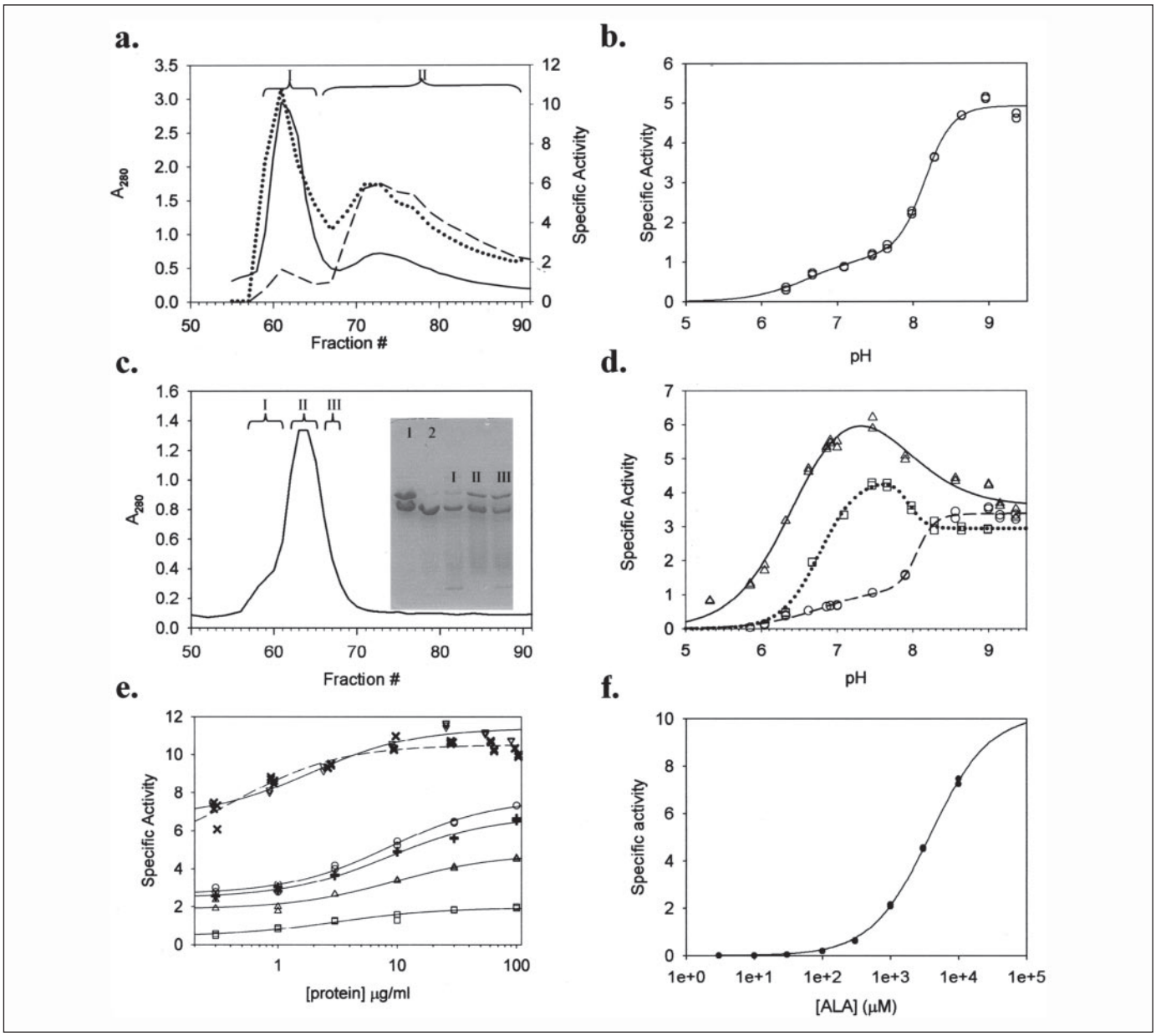

FIGURE 4. **Characterization of R240A.** *a*, Q-Sepharose ion exchange chromatography showing two major protein peaks (*solid line*; A_{280}) with PBGS activity, which are denoted Pools I and II. Specific activity is shown at pH 7 (*dashed line*) and at pH 9 (*dotted line*). *b*, specific activity as a function of pH is presented for Pool I from *a* (5-min assay, 100 μg of protein/assay). *c*, Q-Sepharose rechromatography of Pool II from *a*. The *inset* is a 12% native polyacrylamide gel. *Lane 1*, a mixture of wild-type and F12L proteins showing the octamer and hexamer, respectively; *lane 2*, the R240A hexamer (Pool I from *a* after further purification on Sephacryl S-300); *lanes I–III*, Pools I–III, respectively. *d*, pH-rate profiles of fractions from *c* (15-min assays): fraction 58 (○), fraction 63 (△), and fraction 67 (□). *e*, protein concentration-dependent specific activity of R240A. The assays were carried out for 1 h at pH 9 using ALA concentrations of 1 mM (□), 3 mM (△), 6 mM (+), and 10 mM (○). Assays were carried out for wild-type PBGS (×) and F12L (▽) at 10 mM ALA under the same conditions. The *lines* show the best fit of the data to a three-parameter hyperbolic equation; the *dashed line* shows the fit for the wild-type protein. *f*, determination of K_m and V_{max} at 100 μg/ml R240A during a 60-min assay at pH 9 over a wide range of substrate concentrations. The *solid line* is a fit to the Michaelis-Menten equation.

diluted 10-fold with Q-Sepharose starting buffer, and reapplied to the Q-Sepharose column. Remarkably, the resulting retention time shifted to one more like that of the hexameric form of the protein (Fig. 4*c*). Profiles of specific activity *versus* pH for fractions 58, 63, and 67 in Fig. 4*c* are displayed in Fig. 4*d* and resemble mixtures of the hexameric and octameric morpheeins of human PBGS, with the octamer contaminating the latter half of the peak. Three pools were collected as illustrated in Fig. 4*c*, and native gel electrophoresis (*inset*) of these pools confirmed this interpretation of the kinetic data. The rechromatography data show that the octameric form of R240A is unstable and converts at least partially to the hexamer with time. It is unclear if any misfolded protein also accumulates.

The unexpectedly high activity at pH 7 for fractions 63 and 67 (Fig. 4, *c* and *d*) was proposed to be due to the propensity of human PBGS to favor the octameric structure under assay conditions, as previously observed for PBGS heterohexamers composed of both Phe^{12}- and Leu^{12}-containing subunits (3). The interconversion of the hexamer and octamer, whose structures are illustrated in Fig. 1, is presumed to proceed through a disassembly-reassembly reaction with structural interconversion at the dimer stage of oligomerization. We have already established that a dynamic interconversion of human PBGS morpheeins is facilitated by the molecular motions that accompany catalysis and that active-site ligand binding shifts the equilibrium toward the octamer (3). Conversion of hexameric R240A to the octamer under assay condi-

TABLE 1
Apparent molecular masses of human wild-type and mutant PBGSs
ND, not determined.

	R240A		W19A		Wild-type, pH 7	F12L, pH 7
	pH 7	pH 9	pH 7	pH 9		
Analytical ultracentrifugation						
kDa	188.5 ± 8.8	183.5 ± 5.6	69.6 ± 4.3[a]	ND	244.0 ± 8.9[a,b]	197.9 ± 6.5[b]
Best fit model	2↔6[c]	2↔6	1↔2↔6		2↔6↔8	4↔6
Dynamic light scattering	212.4 ± 1.7	ND	78.6 ± 1.2	81.2 ± 1.7	317.6 ± 20.7	214.4 ± 13.7

[a] Analytical ultracentrifugation measurements were carried out at pH 7.5.
[b] Data were taken from Ref. 1.
[c] The symbol ↔ indicates that the data were fit using equilibrium models.

tions would thus be predicted to result in a time-dependent increase in the specific activity of the R240A protein at pH 7, but not at pH 9 (Fig. 4*d*). The predicted increase at pH 7 was experimentally confirmed (Fig. 5*a*) and fits to an exponential equation with a rather slow rate constant of 0.3 h^{-1}. Equilibrium dialysis of R240A, first into buffer containing ALA, was used to demonstrate that the time-dependent increase in specific activity at pH 7 was indeed due to a shift in the morpheein equilibrium toward the octameric morpheein. Protein samples taken at various times during the dialysis were subjected to native gel electrophoresis. Gels were stained and scanned, and the densitometry data were used to determine the percentage of the protein in the octameric and hexameric states (Fig. 5*b*). The exponential fits of the densitometry data revealed rate constants of 0.12 h^{-1} at pH 7 and 0.39 h^{-1} at pH 9. Dialysis back into buffer without substrate resulted in a slower transition back to the hexamer (Fig. 5*b*), where the rate constants were 0.09 h^{-1} at pH 9 and 0.02 h^{-1} at pH 7. As an additional control, we showed that the specific activity of hexameric R240A did not increase at pH 9 (Fig. 5*a*), although a portion of the protein was converted to an octamer (Fig. 5*b*). The minor decrease in specific activity that was observed at pH 9 may be attributed 1) to a decrease in the concentration of substrate due to a spontaneous dimerization reaction (14), 2) to minor product inhibition, or 3) to the fact that the activity of the hexamer at pH 9 may be higher than that of the octamer.

A size exclusion-purified hexameric form of R240A was further characterized and found to exhibit a protein concentration-dependent specific activity at pH 9 that had not previously been documented for human PBGS (Fig. 4*e*). Because the active sites are wholly contained within the $\alpha\beta$-barrel domain of each subunit, a protein concentration-dependent specific activity indicates that there is a maximally active oligomer that can dissociate or rearrange to smaller, less active species. The apparent K_d for this dissociation/rearrangement falls in the range of 8–9 μg/ml R240A and appears to be independent of the substrate concentration in the range of 3–10 mM ALA (Fig. 4*e*). In contrast, the apparent K_d for F12L is ~2 μg/ml and that for the wild-type PBGS is ~0.5 μg/ml. For wild-type PBGS, this phenomenon is believed to reflect the octamer-hexamer equilibrium that influences wild-type PBGS kinetics at pH 9, but not at pH 7 (1, 3). For F12L, this phenomenon reflects an equilibrium between the hexamer and a smaller, less active species. It is presumed that the plateau seen at low R240A protein concentration (0.3 μg/ml) reflects activity predominantly from the smaller species and that at the highest concentration (100 μg/ml) reflects activity from the largest species, but the stoichiometries of these assemblies are unclear. The R240A data in Fig. 4*e* were fit to the Michaelis-Menten equation and revealed a protein concentration-independent apparent K_m of ~3.7 mM ALA, which is consistent with that previously seen for the human hexameric PBGS mutant F12L (1). However, the four ALA concentrations used in Fig. 4*e* are too high to determine whether there is a quaternary isoform of the protein that exhibits a significantly lower K_m value as might be expected for the octamer. Protein activity data were obtained at an R240A concentration of 100 μg/ml over a wide range of ALA concentrations (Fig. 4*f*). At pH 9, the data fit to a single K_m of 3.8 ± 0.1 mM ALA and a V_{max} of 10.2 ± 0.1 μmol/h/mg and provide no indication for a protein species with a K_m value in the micromolar range. Table 2 shows similar results that were obtained at pH 7 (overnight assays using 30 μg/ml protein), again indicating the absence of structures with a low K_m value. Because an R240A octamer accumulated under assay conditions (Fig. 5), this octamer must not have a sufficiently

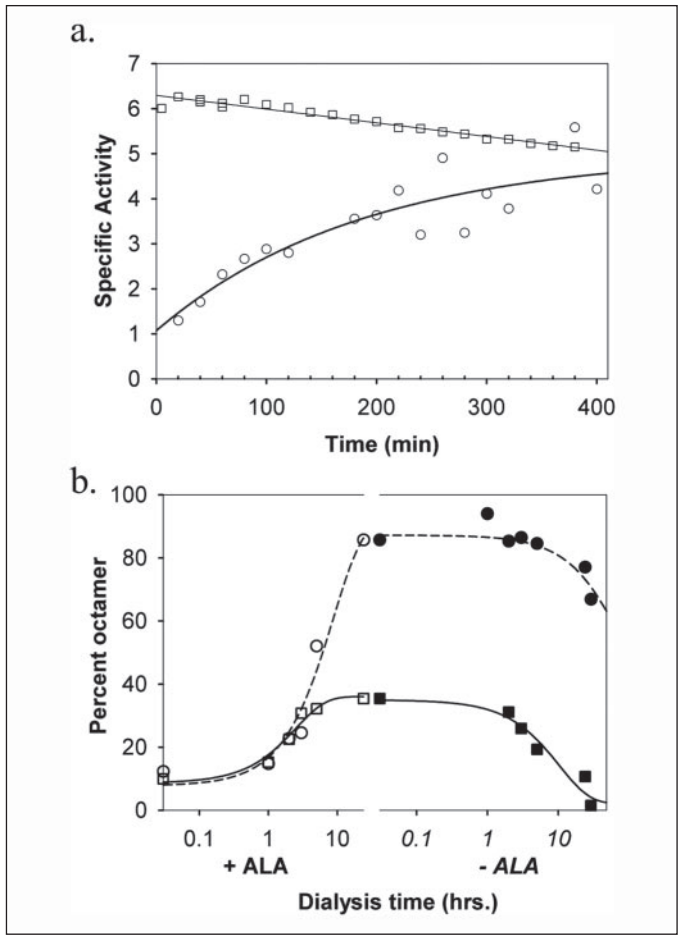

FIGURE 5. **Dynamic equilibration of hexameric and octameric forms of R240A.** *a*, a time-dependent increase in the specific activity of hexameric R240A (10 μg/ml) at pH 7 (○) is consistent with a substrate-mediated shift in the morpheein equilibrium from the lower activity hexamer to the higher activity octamer. At pH 9 (□), R240A (10 μg/ml) suffered a slight loss in activity with time (see "Results"). *b*, equilibrium dialysis was performed, starting with hexameric R240A (1.8 mg/ml) dialyzed at 37 °C against assay buffer containing 10 mM ALA (*open symbols*) for 24 h, after which time the protein was dialyzed back into buffer without ALA (*closed symbols*). *Circles* represent the experiment at pH 7; *squares* represent the experiment at pH 9. The percent octamer was determined by densitometry measurements of native gels (3). The *lines* are fits to a simple exponential equation.

TABLE 2

Kinetic parameters K_m (mM) and V_{max} (μmol/h/mg) for human wild-type and mutant PBGSs

ND, not determined.

Parameter	pH	F12L[a,b]	Wild-type[a,b]	R240A[c]	W19A[d]	
					High activity form	Low activity form
K_{m1}	7		0.25 ± 0.01			
V_{max1}	7		55.5 ± 0.2			
K_{m2}	7	17.7 ± 1.1		6.92 ± 0.35	ND	ND
V_{max2}	7	1.14 ± 0.05		3.56 ± 0.09	ND	ND
K_{m1}	9		0.015 ± 0.01			
V_{max1}	9		8.16 ± 0.13			
K_{m2}	9	4.6 ± 0.1	4.46 ± 0.80	3.8 ± 0.1	4.36 ± 0.27	5.02 ± 0.28
V_{max2}	9	18.2 ± 0.2	6.67 ± 0.36	10.2 ± 0.1	18.29 ± 0.52	9.76 ± 0.25

[a] Data are taken from Ref. 3.
[b] K_{m1} and K_{m2} reflect the K_m values for the octamer and hexamer, respectively. For the wild-type protein at pH 9, these oligomers are in equilibrium, and the kinetic parameters derive from a fit of the data to a double hyperbolic equation (1, 3).
[c] The R240A data, which fit to a single hyperbolic equation, nevertheless are seen to represent a dynamic conversion of hexamer to octamer during the assay.
[d] The W19A data also fit to a single hyperbolic and appear to represent catalysis by dimers.

low K_m value to cause a deviation from simple saturation kinetic behavior (see "Discussion").

Human PBGS Mutant W19A—The purification of W19A followed a reported procedure (3) through the Q-Sepharose column step, where one broad peak of protein exhibited PBGS activity (Fig. 6*a*). SDS gels show a high level of purity throughout the peak, and native gels show a diffuse major band running near the bottom of a 12.5% gel, suggesting a low aggregation state (see below). The specific activity measurements support that this peak contained two different quaternary isoforms with different specific activities (Fig. 6*a*). Based on these different specific activities, two forms of W19A were pooled from fractions 10–12 and 16–18 (named Pools I and II respectively), and they were further purified on Sephacryl S-300 (Fig. 6*b*). The major components of the two forms eluted from the Sephacryl S-300 column at the same retention time, and there was a minor component observed in Pool II. Analytical ultracentrifugation data (loading concentration of 0.29 mg/ml) on samples similar to the major component but from a previous purification showed that Pool I consisted predominantly of dimers (90%) at pH 7.5, with the remaining protein existing as monomers (Table 1). To further support the size of the proteins in each of these pools, the elution volume of various human PBGS preparations on the Sephacryl S-300 column is plotted for an octamer (wild-type), hexamer (F12L), tetramer (the minor component from W19A Pool II), and dimer (the major component from W19A Pools I and II) (Fig. 6*b*, *inset*); these data show the expected linear relationship between the elution volume and log molecular mass, further supporting the dimeric and tetrameric nature of the W19A components. No distinct protein peak was observed at ~210 ml, the expected elution volume of the monomer, although a minor monomeric component would be masked in the tail of the dimer peak. Native and SDS gels are also presented (Fig. 6*c*). The native gel shows separation of the wild-type octamer, the F12L hexamer, the putative tetrameric minor component of W19A, and the two dimeric forms of W19A (which run side by side). The SDS gel shows equivalent subunit molecular mass for all these human PBGS morpheeins. Dynamic light scattering measurement also confirmed that, at 1 mg/ml, the apparent molecular mass of W19A Pool I is that of a dimer at both pH 7 and 9 (Table 1).

To further characterize the dimeric forms of W19A, the pH-rate profiles of Pools I and II were determined (Fig. 6*d*); neither expressed any significant activity at pH 7, and both fit well to an apparent two-proton pK_a of 8.3. Both forms showed significant protein concentration-dependent specific activity at pH 9 (Fig. 6*e*). The protein concentration dependence for the low activity form (Pool II) fits well to a simple hyperbolic association model in which the smaller, less active form (presumably monomer) is inactive. The best fit of the protein concentration for the high activity form (Pool I) suggests that there may be a monomeric form of human PBGS with measurable activity (*solid line* in Fig. 6*e*). Substrate saturation data for both forms, when assayed at pH 9 in the range of 3 μM to 10 mM ALA, fit to a simple hyperbolic equation, which again showed no indication of a low K_m form (Fig. 6*f*). The high activity form (Pool I) has a K_m value of 4.36 ± 0.27 mM (at 45 μg/ml protein), and the low activity form (Pool II) has a comparable K_m value of 5.02 ± 0.28 mM (at 35 μg/ml protein). Equilibrium dialysis of both the W19A dimers showed that these proteins do not assemble into either the hexamer or octamer as a consequence of substrate binding and turnover.

DISCUSSION

This study has addressed the contribution of two critical intersubunit interactions to the thermodynamics that determine the outcome of the folding and assembly of human PBGS. As predicted by the analogy of the role of Arg^{240} with that of the allosteric magnesium of some PBGS proteins (Fig. 2), the morpheein equilibrium for the human PBGS mutant R240A lies far toward the hexamer, but not so far as to overcome the energetic stabilization afforded the octameric morpheein by substrate binding and/or turnover. This is different from the naturally occurring F12L hexamer, which does not show any propensity to form a homomeric octamer, although hetero-octamers can exist in concert with the wild-type protein (1, 3). In the absence of additional crystal structures, it is not possible to say why the F12L hexamer is stable, whereas the R240A hexamer is metastable; however, the ready interconversion of the R240A hexamer and octamer supports the hypothesis that the energy difference between these two states is small. Furthermore, a potential physiological significance arises from our knowledge that human wild-type PBGS exists predominantly as a homo-octamer, but can equilibrate with a functionally distinct wild-type homohexamer in the presence of substrate at high pH values (1, 3). Also as predicted from the common role of Trp^{19} in dimer-dimer association for both the hexamer and octamer (Fig. 3), the human PBGS mutant W19A assembles into the dimeric state, even in the presence of substrate. Somewhat unexpected was the observation of two different dimeric states for W19A, both of which appear to be stable with no measurable propensity to oligomerize further.

The structures of human wild-type PBGS and the F12L mutant have been solved by x-ray crystallography (Protein Data Bank codes 1E51 and 1PV8, respectively) and are shown in Fig. 1 (1, 15). Both of these structures show considerable regions of disorder, but the different assemblies are incontrovertible. The high pH optimum and high K_m for the F12L hexamer have both been attributed to the more open conformations of the active-site lid as reflected by disorder in the crystal structure (2, 16). In the wild-type structure, residues from the closed active-site lid inter-

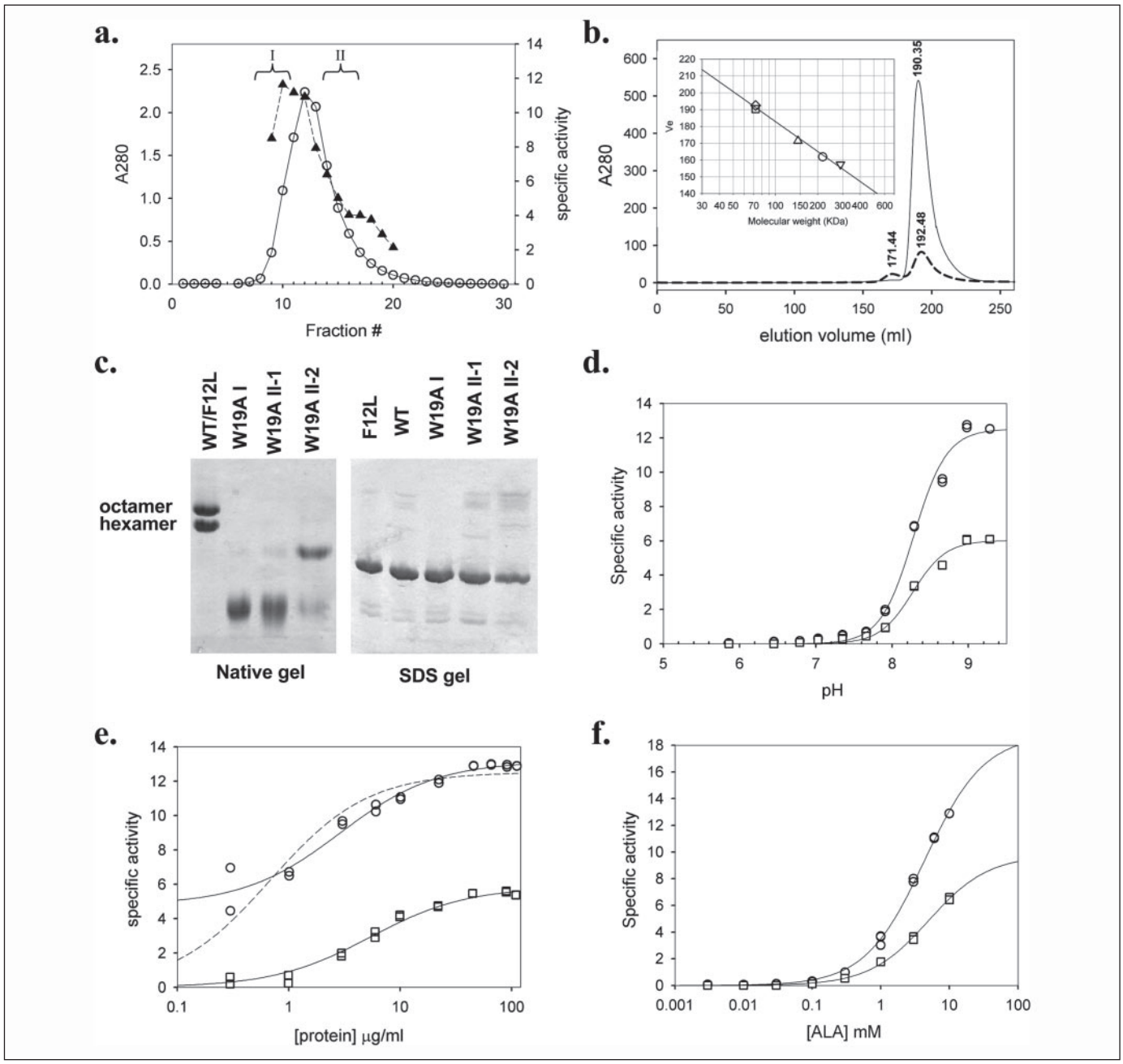

FIGURE 6. **Characterization of W19A.** *a*, Q-Sepharose purification showing the W19A protein (○; A_{280}) and its specific activity (▲) at pH 9. *b*, gel filtration on Sephacryl S-300 showing elution of Pool I (*solid line*) and Pool II (*dashed line*). The *inset* is a plot of the elution volume (V_e) for various forms of human PBGS, including the wild-type octamer (▽), the F12L hexamer (○), W19A Pool I plotted as a dimer (◇), W19A Pool II plotted as a dimer (□), and the minor putatively tetrameric component in W19A Pool II (△). *c*, 12.5% native and SDS-polyacrylamide gels showing wild-type PBGS (*WT*; octamer), F12L (hexamer), and the W19A pools illustrated in *b*. *W19A I* is the peak eluting at 190.35 ml, *W19A II-1* is the peak eluting at 192.48 ml, and *W19A II-2* is the peak eluting at 174.44 ml. *d*, pH-rate profiles of the high activity form (Pool I (○), 36 μg/ml) and the low activity dimeric form (Pool II-1 (□), 39 μg/ml) of W19A. The *lines* indicate the best fit of the data to a two-proton pK_a. *e*, protein concentration-dependent specific activity at pH 9 for Pool I (○) and Pool II-1 (□) of W19A. Pool I data fit best to a three-parameter hyperbolic equation (*solid line*) and less well to a two-parameter hyperbolic equation (*dashed line*). Pool II-1 data are fit to a two-parameter hyperbolic (*solid line*) (see "Discussion"). *f*, determination of K_m and V_{max} values for Pool I (○; 45 μg/ml) and Pool II-1 (□; 35 μg/ml) at pH 9. The *lines* are fits of the kinetic data to the Michaelis-Menten equation.

act with the N-terminal arm of the neighboring subunit in the hugging dimer. The more solvent-accessible active site of the F12L hexamer is proposed to necessitate a higher pH to facilitate a Schiff base formation that is required for product formation; the high K_m is attributed to the loss of key interactions between the lid residues and the K_m-determining substrate molecule (2, 5, 16). Most of the human PBGS morpheeins described herein, which are the R240A hexamer and both W19A dimers, share with the F12L hexamer the kinetic characteristics of an alkaline pH optimum of ~9 and a K_m of ~5 mM at that pH. Thus, we propose that these morpheeins also contain an active site that is more solvent-accessible than that of the wild-type octamer. In the R240A hexamer, we can presume that the solvent accessibility is similar to that in F12L, where the active-site lid is less able to sequester the active site from bulk solvent. In W19A, however, the solvent accessibility may arise from leakage at the base of the active site, where Trp^{19} normally penetrates, like a plug in the bottom of a barrel. X-ray crystallographic analysis may help to determine the structural differences between these PBGS morpheeins, but it is our experience that PBGS proteins that

appear to readily equilibrate between morpheein structures are resistant to forming diffraction quality crystals.

Based on similar mobility on native gels and the common retention time on the gel filtration column, both forms of W19A appear to be dimeric, and we presume that the difference lies in the orientation of the N-terminal arms relative to the $\alpha\beta$-barrels. Because both forms have a K_m value similar to that of F12L at pH 9 ($K_m = 4.6 \pm 0.1$ mM (1, 3)), we presume that the N-terminal arms are not in position to stabilize the active-site lids through the arm-hugging-barrel interaction seen in the wild-type hugging dimer and octamer structures (Fig. 1*a*). Thus, we do not predict that either W19A dimer is equivalent to the hugging dimer component of the octameric assembly. Because a closed active site requires two different arm-barrel interactions (one stabilizing the lid and another plugging the base), any dimeric form of W19A would be predicted to contain a solvent-accessible active site, which is confirmed by the observed high pH optimum (Fig. 6*d*). More intriguing is the protein concentration dependence of the high activity form of W19A, where the best fit of the data suggests that the smaller form (presumably monomeric) may be active (Fig. 6*e*). X-ray crystal structure analysis of the purified W19A dimers may shed additional light on this possibility.

Mutation of the human PBGS gene is associated with a disease known as Doss porphyria, which is one of a complex variety of porphyric disorders (17) that has not been previously associated with alterations in protein folding/assembly. In most cases, a single mutation to only one allele encoding PBGS does not result in a disease state, even though enzyme activity may be reduced to <50% of normal (18). For instance, individuals heterozygous for F12L are not porphyric. Instead, most cases of Doss porphyria occur in individuals who carry two different aberrant PBGS-encoding genes. In these patients, the documented mutations include E89K, C132R, G133R, V153M, R240W, A274T, and V275M (19–22), the first three of which are near enough to the active-site zinc to disrupt its function. In the wild-type octamer (Protein Data Bank code 1E51), Glu^{89} becomes ordered when the catalytic zinc is bound; Cys^{132} is a ligand to the catalytic zinc ion, and Gly^{133} is adjacent to Cys^{132}. Some of the other naturally occurring variants may contribute to porphyria by shifting the folding and assembly of human PBGS away from the octameric state. For instance, the R240W mutation may destabilize the octamer similarly to the R240A variant discussed herein, and both Ala^{274} and Val^{275} are near those residues that interact directly with Trp^{19} of an adjacent dimer in both the octameric and hexameric assemblies. To date, the concept of conformational disease has been limited to prion-like phenomena, but may also apply to physiological dysregulations based on mutations that alter a normal physiologically significant equilibration of morpheeins. Ongoing studies are addressing these possibilities.

REFERENCES

1. Breinig, S., Kervinen, J., Stith, L., Wasson, A. S., Fairman, R., Wlodawer, A., Zdanov, A., and Jaffe, E. K. (2003) *Nat. Struct. Biol.* **10,** 757–763
2. Jaffe, E. K. (2005) *Trends Biochem. Sci.* **30,** 490–497
3. Tang, L., Stith, L., and Jaffe, E. K. (2005) *J. Biol. Chem.* **280,** 15786–15793
4. Frankenberg, N., Erskine, P. T., Cooper, J. B., Shoolingin-Jordan, P. M., Jahn, D., and Heinz, D. W. (1999) *J. Mol. Biol.* **289,** 591–602
5. Kervinen, J., Jaffe, E. K., Stauffer, F., Neier, R., Wlodawer, A., and Zdanov, A. (2001) *Biochemistry* **40,** 8227–8236
6. Jaffe, E. K., Ali, S., Mitchell, L. W., Taylor, K. M., Volin, M., and Markham, G. D. (1995) *Biochemistry* **34,** 244–251
7. Jaffe, E. K. (2003) *Chem. Biol.* **10,** 25–34
8. Jaffe, E. K., Volin, M., Bronson-Mullins, C. R., Dunbrack, R. L., Jr., Kervinen, J., Martins, J., Quinlan, J. F., Jr., Sazinsky, M. H., Steinhouse, E. M., and Yeung, A. T. (2000) *J. Biol. Chem.* **275,** 2619–2626
9. Jordan, P. M., and Gibbs, P. N. (1985) *Biochem. J.* **227,** 1015–1020
10. Wu, J. W., Hu, M., Chai, J., Seoane, J., Huse, M., Li, C., Rigotti, D. J., Kyin, S., Muir, T. W., Fairman, R., Massague, J., and Shi, Y. (2001) *Mol. Cell* **8,** 1277–1289
11. Laue, T., Shaw, B. D., Ridgeway, T. M., and Pelletier, S. L. (1992) in *Biochemistry and Polymer Science* (Harding, S. E., Rowe, A., and Horton, J. C., eds) pp. 90–125, Royal Society of Chemistry, Cambridge
12. Arkin, M., and Lear, J. D. (2001) *Anal. Biochem.* **299,** 98–107
13. van Holde, K. E., Johnson, C., and Ho, P. S. (1998) *Principles of Physical Biochemistry*, Prentice-Hall, Englewood Cliffs, NJ
14. Jaffe, E. K., and Rajagopalan, J. S. (1990) *Bioorg. Chem.* **18,** 381–394
15. Mills-Davies, N. L. (2000) *Structure of Human Erythrocyte 5-Aminolaevulinic Acid Dehydratase, the Second Enzyme in the Biosynthesis Pathway of Haem.* Ph.D. thesis, University of Southampton, Southampton, UK
16. Jaffe, E. K. (2004) *Bioorg. Chem.* **32,** 316–325
17. Sassa, S., and Kappas, A. (2000) *J. Intern. Med.* **247,** 169–178
18. Maruno, M., Furuyama, K., Akagi, R., Horie, Y., Meguro, K., Garbaczewski, L., Chiorazzi, N., Doss, M. O., Hassoun, A., Mercelis, R., Verstraeten, L., Harper, P., Floderus, Y., Thunell, S., and Sassa, S. (2001) *Blood* **97,** 2972–2978
19. Akagi, R., Nishitani, C., Harigae, H., Horie, Y., Garbaczewski, L., Hassoun, A., Mercelis, R., Verstraeten, L., and Sassa, S. (2000) *Blood* **96,** 3618–3623
20. Akagi, R., Shimizu, R., Furuyama, K., Doss, M. O., and Sassa, S. (2000) *Hepatology* **31,** 704–708
21. Sassa, S., Ishida, N., Fujita, H., Fukuda, Y., Noguchi, T., Doss, M., and Kappas, A. (1992) *Trans. Assoc. Am. Physicians* **105,** 250–259
22. Akagi, R., Kato, K., Inoue, R., Anderson, K. E., Jaffe, E. K., and Sassa, S. (2006) *Mol. Genet. Metab.* 10.1016/j.ymgme.2005.10.011